

# CONVERGENCE OF LAGRANGE FINITE ELEMENTS FOR THE MAXWELL EIGENVALUE PROBLEM IN 2D

DANIELE BOFFI, JOHNNY GUZMÁN, AND MICHAEL NEILAN

**ABSTRACT.** We consider finite element approximations of the Maxwell eigenvalue problem in two dimensions. We prove, in certain settings, convergence of the discrete eigenvalues using Lagrange finite elements. In particular, we prove convergence in three scenarios: piecewise linear elements on Powell–Sabin triangulations, piecewise quadratic elements on Clough–Tocher triangulations, and piecewise quartics (and higher) elements on general shape-regular triangulations. We provide numerical experiments that support the theoretical results. The computations also show that, on general triangulations, the eigenvalue approximations are very sensitive to nearly singular vertices, i.e., vertices that fall on exactly two “almost” straight lines.

## 1. INTRODUCTION

Let  $\Omega \subset \mathbb{R}^2$  be a contractible polygonal domain and consider the eigenvalue problem

$$(1.1) \quad (\operatorname{rot} \mathbf{u}, \operatorname{rot} \mathbf{v}) = \eta^2(\mathbf{u}, \mathbf{v}) \quad \forall \mathbf{v} \in \mathbf{H}_0(\operatorname{rot}, \Omega),$$

where  $\mathbf{H}(\operatorname{rot}, \Omega) := \{\mathbf{v} \in \mathbf{L}^2(\Omega) : \operatorname{rot} \mathbf{v} \in L^2(\Omega)\}$ ,  $\mathbf{H}_0(\operatorname{rot}, \Omega) := \{\mathbf{v} \in \mathbf{H}(\operatorname{rot}, \Omega) : \mathbf{v} \cdot \mathbf{t} = 0 \text{ on } \partial\Omega\}$ , and  $(\cdot, \cdot)$  denotes the  $L^2$  inner product over  $\Omega$ . Given a finite element space  $\hat{\mathbf{V}}_h \subset \mathbf{H}_0(\operatorname{rot}, \Omega)$ , a finite element method seeks  $\mathbf{u}_h \in \hat{\mathbf{V}}_h \setminus \{0\}$  and  $\eta_h \in \mathbb{R}$  satisfying

$$(1.2) \quad (\operatorname{rot} \mathbf{u}_h, \operatorname{rot} \mathbf{v}_h) = \eta_h^2(\mathbf{u}_h, \mathbf{v}_h) \quad \forall \mathbf{v}_h \in \hat{\mathbf{V}}_h.$$

For example, one can take  $\hat{\mathbf{V}}_h$  to be the  $\mathbf{H}_0(\operatorname{rot}; \Omega)$ -conforming Nedelec finite elements (i.e., the rotated Raviart–Thomas finite elements) as the finite element space. It is well-known this choice leads to a convergent approximation of the eigenvalue problem. On the other hand, taking  $\hat{\mathbf{V}}_h$  as a space continuous piecewise polynomials (i.e., a  $\mathbf{H}^1(\Omega)$ -conforming Lagrange finite element) may lead to spurious eigenvalues for any mesh parameter.

There is a vast literature on this subject. The interested reader is referred to [5, Section 20] for an extensive survey including a comprehensive list of references about Nedelec finite elements and to [8, 6] for a discussion about the use of standard Lagrange finite elements (see also [3] for a discussion of these phenomena in the context of the finite element exterior calculus).

To better appreciate the problem and its discretization, we consider the equivalent formulation introduced in [8] for  $\eta \neq 0$ :

$$(1.3a) \quad (\boldsymbol{\sigma}, \boldsymbol{\tau}) + (p, \operatorname{rot} \boldsymbol{\tau}) = 0 \quad \forall \boldsymbol{\tau} \in \mathbf{H}_0(\operatorname{rot}, \Omega),$$

$$(1.3b) \quad (\operatorname{rot} \boldsymbol{\sigma}, q) = -\lambda(p, q) \quad \forall q \in L_0^2(\Omega).$$

Taking  $q = \operatorname{rot} \mathbf{v}$  with  $\mathbf{v} \in \mathbf{H}_0(\operatorname{rot}, \Omega)$  shows the equivalence of (1.3) and (1.1) with  $\boldsymbol{\sigma} = \mathbf{u}$ ,  $\lambda = \eta^2$ , and  $p = -\frac{1}{\lambda} \operatorname{rot} \mathbf{u}$ .

---

The first author is a member of the INdAM Research group GNCS and his research is partially supported by IMATI/CNR and by PRIN/MIUR. The second author is partially supported by the NSF grant DMS-1620100. The third author is partially supported by the NSF grant DMS-1719829.

The corresponding finite element method for the mixed formulation (1.3) seeks  $\sigma_h \in \mathring{\mathbf{V}}_h \setminus \{0\}$ ,  $p_h \in \mathring{Q}_h$ , and  $\lambda_h \in \mathbb{R}$  such that

$$(1.4a) \quad (\sigma_h, \tau_h) + (p_h, \text{rot } \tau_h) = 0, \quad \forall \tau \in \mathring{\mathbf{V}}_h,$$

$$(1.4b) \quad (\text{rot } \sigma_h, q_h) = -\lambda_h (p_h, q_h) \quad \forall q_h \in \mathring{Q}_h$$

with  $\mathring{Q}_h \subset L_0^2(\Omega)$ . Similar to the continuous problem, if the finite element spaces satisfy  $\text{rot } \mathring{\mathbf{V}}_h \subset \mathring{Q}_h$ , then the mixed finite element formulation (1.4) is equivalent to the primal one (1.2) with  $\sigma_h = \mathbf{u}_h$ ,  $\lambda_h = \eta_h^2$  and  $p_h = -\frac{1}{\lambda} \text{rot } \mathbf{u}_h$ .

If  $\mathring{\mathbf{V}}_h$  is the Nedelec space of index  $k$ , then we may take  $\mathring{Q}_h$  to be the space of piecewise polynomials of degree  $k-1$ . In this case,  $(\mathring{\mathbf{V}}_h, \mathring{Q}_h)$  forms an inf-sup stable pair of spaces, in particular, there exists a Fortin projection

$$\Pi_V : \mathring{\mathbf{V}} \rightarrow \mathring{\mathbf{V}}_h$$

satisfying

$$(1.5a) \quad \text{rot } \Pi_V \tau = \Pi_Q \text{rot } \tau \quad \forall \tau \in \mathring{\mathbf{V}},$$

$$(1.5b) \quad \|\Pi_V \tau - \tau\|_{L^2(\Omega)} \leq Ch^{1/2+\delta} (\|\tau\|_{H^{1/2+\delta}(\Omega)} + \|\text{rot } \tau\|_{L^2(\Omega)}) \quad \forall \tau \in \mathring{\mathbf{V}}.$$

Here  $\mathring{\mathbf{V}} := \mathbf{H}_0(\text{rot}, \Omega) \cap \mathbf{H}(\text{div}, \Omega)$ . Moreover,  $\delta \in (0, 1/2]$  is a parameter such that  $\mathring{\mathbf{V}} \hookrightarrow \mathbf{H}^{1/2+\delta}(\Omega)$  [2], and  $\Pi_Q : L_0^2(\Omega) \rightarrow \mathring{Q}_h$  is the  $L^2$  orthogonal projection onto  $\mathring{Q}_h$ . Using this projection one can prove that the corresponding source problems converges uniformly, and this is sufficient to prove convergence of the eigenvalue problem (1.2) (see [18, 5] and Proposition 2.1).

On the other hand, if  $\mathring{\mathbf{V}}_h$  is taken to be the Lagrange finite element space of degree  $k$ , then a natural choice of  $\mathring{Q}_h$  is the space of (discontinuous) piecewise polynomials of degree  $k-1$ . However,  $(\mathring{\mathbf{V}}_h, \mathring{Q}_h)$  is *not* inf-sup stable on generic triangulations, at least when  $k=1$  [21, 7], and therefore there does not exist a Fortin projection satisfying (1.5). On the other hand, the pair  $(\mathring{\mathbf{V}}_h, \mathring{Q}_h)$  is known to be stable on special triangulations, even if the inf-sup condition might not be sufficient to guarantee the existence of a Fortin projector satisfying (1.5) (see [6]). On very special triangulations, Wong and Cendes [24] showed numerically that solutions to (1.2) do converge to the correct eigenvalues using piecewise linear Lagrange elements (i.e.,  $k=1$ ). In fact, they used precisely the Powell–Sabin triangulations (see Figure 1). In this paper, we prove that indeed using Lagrange elements in conjunction with Powell–Sabin triangulation leads to a convergent method. We do this by proving that there is a Fortin projection of sorts. We show that there exists an operator  $\Pi_V : \mathring{\mathbf{V}}(Q_h) \rightarrow \mathring{\mathbf{V}}_h$  satisfying

$$(1.6a) \quad \text{rot } \Pi_V \tau = \text{rot } \tau \quad \forall \tau \in \mathring{\mathbf{V}}(Q_h),$$

$$(1.6b) \quad \|\Pi_V \tau - \tau\|_{L^2(\Omega)} \leq Ch^{1/2+\delta} (\|\tau\|_{H^{1/2+\delta}(\Omega)} + \|\text{rot } \tau\|_{L^2(\Omega)}), \quad \forall \tau \in \mathring{\mathbf{V}}(Q_h),$$

where  $\mathring{\mathbf{V}}(Q_h) = \{\mathbf{v} \in \mathring{\mathbf{V}} : \text{rot } \mathbf{v} \in \mathring{Q}_h\}$ . Note that (1.5) implies (1.6), and we prove convergence of the eigenvalue problem whenever there is a projection  $\Pi_V$  satisfying (1.6). In addition to linear Lagrange elements on Powell–Sabin triangulations, we prove the existence of such a projection on Clough–Tocher splits using quadratic Lagrange elements, and on general triangulations using  $k$ th degree Lagrange elements with  $k \geq 4$  (i.e., the Scott–Vogelius finite elements). For the Scott–Vogelius finite elements, we find the approximate eigenvalues are extremely sensitive if the mesh has nearly singular vertices, i.e., vertices that fall on exactly two “almost” straight lines (cf. Section 3.3). We give numerical examples that illustrate this behavior.

Recently Duan et al. [12] considered Lagrange finite elements for Maxwell’s eigenvalue problem in two and three dimensions. However, they use a different formulation than ours and they also add a stabilization term.

The paper is organized as follows: In the next section we give a convergence proof for finite elements spaces with stable projections. In Section 3, we provide three examples of Lagrange finite element spaces with stable projections: the piecewise linear Lagrange space on Powell–Sabin splits, the

piecewise quadratic Lagrange space on Clough–Tocher splits, and the piecewise  $k$ th degree Lagrange space on generic triangulations. Finally, in Section 4 we provide numerical experiments.

## 2. CONVERGENCE FRAMEWORK

Define the two-dimensional **curl**, **rot**, and divergence operators as

$$\mathbf{curl} u = \left( \frac{\partial u}{\partial x_2}, -\frac{\partial u}{\partial x_1} \right)^\top, \quad \mathbf{rot} \mathbf{v} = \frac{\partial v_2}{\partial x_1} - \frac{\partial v_1}{\partial x_2}, \quad \mathbf{div} \mathbf{v} = \frac{\partial v_1}{\partial x_1} + \frac{\partial v_2}{\partial x_2},$$

and define the Hilbert spaces

$$\begin{aligned} \mathbf{H}_0(\mathbf{rot}, \Omega) &= \{ \mathbf{v} \in \mathbf{L}^2(\Omega) : \mathbf{rot} \mathbf{v} \in L^2(\Omega), \mathbf{v} \cdot \mathbf{t}|_{\partial\Omega} = 0 \}, \\ \mathbf{H}(\mathbf{div}, \Omega) &= \{ \mathbf{v} \in \mathbf{L}^2(\Omega) : \mathbf{div} \mathbf{v} \in L^2(\Omega) \}, \end{aligned}$$

where  $\mathbf{t}$  is a unit tangent vector of  $\partial\Omega$ . Recall that  $\mathring{\mathbf{V}} = \mathbf{H}_0(\mathbf{rot}, \Omega) \cap \mathbf{H}(\mathbf{div}, \Omega)$ .

Let  $\mathring{\mathbf{V}}_h \subset \mathbf{H}_0(\mathbf{rot}, \Omega)$  and  $\mathring{Q}_h \subset L_0^2(\Omega)$  be finite element spaces such that  $\mathbf{rot} \mathring{\mathbf{V}}_h \subset \mathring{Q}_h$ .

**2.1. Source problems.** We will require the corresponding source problems for the analysis. To this end, we define the solution operators  $\mathbf{A} : L^2(\Omega) \rightarrow \mathbf{H}_0(\mathbf{rot}, \Omega)$  and  $T : L^2(\Omega) \rightarrow L_0^2(\Omega)$  such that for given  $f \in L^2(\Omega)$ , there holds

$$(2.1a) \quad (\mathbf{A}f, \boldsymbol{\tau}) + (Tf, \mathbf{rot} \boldsymbol{\tau}) = 0, \quad \forall \boldsymbol{\tau} \in \mathbf{H}_0(\mathbf{rot}, \Omega),$$

$$(2.1b) \quad (\mathbf{rot} \mathbf{A}f, q) = (f, q) \quad \forall q \in L_0^2(\Omega).$$

Likewise, the discrete source problem is given by: Find  $\mathbf{A}_h f \in \mathring{\mathbf{V}}_h$  and  $T_h f \in \mathring{Q}_h$  such that

$$(2.2a) \quad (\mathbf{A}_h f, \boldsymbol{\tau}_h) + (T_h f, \mathbf{rot} \boldsymbol{\tau}_h) = 0 \quad \forall \boldsymbol{\tau}_h \in \mathring{\mathbf{V}}_h,$$

$$(2.2b) \quad (\mathbf{rot} \mathbf{A}_h f, q_h) = (f, q_h) \quad \forall q_h \in \mathring{Q}_h.$$

Note that  $\mathbf{A}f = \mathbf{curl} Tf$ , and so  $\mathbf{div} \mathbf{A}f = 0$ . Moreover, using that  $\mathbf{rot} \mathbf{A}f = f$  we have that  $\mathbf{A}f \in \mathring{\mathbf{V}}$ .

We define the operator norm:

$$(2.3) \quad \|T - T_h\| := \sup_{f \in L^2(\Omega) \setminus \{0\}} \frac{\|(T - T_h)f\|_{L^2(\Omega)}}{\|f\|_{L^2(\Omega)}}.$$

We will use the next standard result that states that the uniform convergence of the discrete source problem implies convergence of the discrete eigenvalues. This result is a consequence of the classical discussion in [4, Section 8] (see also [5, Section 9] and [8, Theorem 4.4]).

**Proposition 2.1.** *Let  $T$  and  $T_h$  be defined from (2.1) and (2.2), respectively, and suppose that  $\|T - T_h\| \rightarrow 0$  as  $h \rightarrow 0$ . Consider the problem (1.3) and consider the nonzero eigenvalues  $0 < \lambda^{(1)} \leq \lambda^{(2)} \leq \dots$ . Consider also (1.4) and its non-zero eigenvalues  $0 < \lambda_h^{(1)} \leq \lambda_h^{(2)} \leq \dots$ . Then, for any fixed  $i$ ,  $\lim_{h \rightarrow 0} \lambda_h^{(i)} = \lambda^{(i)}$ .*

Therefore, to prove convergence of eigenvalues it suffices to show uniform convergence of the discrete source problem. To prove this, we will exploit the embedding  $\mathring{\mathbf{V}} \hookrightarrow \mathbf{H}^{1/2+\delta}(\Omega)$  along with an assumption on the finite element spaces. The embedding result is proved in three dimensions in [2], and we state the two dimensional version here.

**Proposition 2.2.** *Let  $\Omega$  be a contractible polygonal domain. Then there exists constants  $\delta \in (0, 1/2]$  and  $C > 0$  such that*

$$\|\mathbf{v}\|_{\mathbf{H}^{1/2+\delta}(\Omega)} \leq C(\|\mathbf{div} \mathbf{v}\|_{L^2(\Omega)} + \|\mathbf{rot} \mathbf{v}\|_{L^2(\Omega)}) \quad \forall \mathbf{v} \in \mathring{\mathbf{V}}.$$

From now on  $\delta$  will refer to the delta of the above proposition. We will use the following space

$$(2.4) \quad \mathring{\mathbf{V}}(Q_h) = \{ \boldsymbol{\tau} \in \mathring{\mathbf{V}} : \mathbf{rot} \boldsymbol{\tau} \in \mathring{Q}_h \}.$$

**Assumption 2.3.** We assume that  $\text{rot } \mathring{\mathbf{V}}_h \subset \mathring{\mathbf{Q}}_h$  and the existence of a projection  $\mathbf{\Pi}_V : \mathring{\mathbf{V}}(Q_h) \rightarrow \mathring{\mathbf{V}}_h$  such that

$$(2.5a) \quad \text{rot } \mathbf{\Pi}_V \boldsymbol{\tau} = \text{rot } \boldsymbol{\tau} \quad \forall \boldsymbol{\tau} \in \mathring{\mathbf{V}}(Q_h),$$

$$(2.5b) \quad \|\mathbf{\Pi}_V \boldsymbol{\tau} - \boldsymbol{\tau}\|_{L^2(\Omega)} \leq \omega_0(h)(\|\boldsymbol{\tau}\|_{H^{1/2+\delta}(\Omega)} + \|\text{rot } \boldsymbol{\tau}\|_{L^2(\Omega)}) \quad \forall \boldsymbol{\tau} \in \mathring{\mathbf{V}}(Q_h).$$

Furthermore, we assume that the  $L^2$ -orthogonal projection  $\mathbf{\Pi}_Q : L^2(\Omega) \rightarrow \mathring{\mathbf{Q}}_h$  satisfies

$$\|\mathbf{\Pi}_Q \phi - \phi\|_{L^2(\Omega)} \leq \omega_1(h) \|\mathbf{curl} \phi\|_{L^2(\Omega)} \quad \forall \phi \in H^1(\Omega) \cap L_0^2(\Omega).$$

Here, the constants are assumed to satisfy  $\omega_0(h), \omega_1(h) > 0$  and  $\lim_{h \rightarrow 0^+} \omega_i(h) = 0$  for  $i = 0, 1$ .

**Theorem 2.4.** Suppose that  $(\mathring{\mathbf{V}}_h, \mathring{\mathbf{Q}}_h)$  satisfy Assumption 2.3. Let  $T$  and  $T_h$  be defined by (2.1) and (2.2), respectively. Then there holds

$$\|T - T_h\| \leq C(\omega_0(h) + \omega_1(h)).$$

Note that Theorem 2.4 and Proposition 2.1 imply that the discrete eigenvalues in the finite element method (1.2) converge to the correct values. To prove Theorem 2.4, we require two preliminary results.

**Lemma 2.5.** Suppose that Assumption 2.3 is satisfied. Then there exists a constant  $C > 0$  such that

$$\|\mathbf{A}\mathbf{\Pi}_Q f - \mathbf{A}f\|_{L^2(\Omega)} + \|T\mathbf{\Pi}_Q f - Tf\|_{L^2(\Omega)} \leq C\omega_1(h)\|f\|_{L^2(\Omega)} \quad \forall f \in L^2(\Omega).$$

*Proof.* Let  $f \in L^2(\Omega)$  and set  $\boldsymbol{\sigma} = \mathbf{A}f, u = Tf, \boldsymbol{\psi} = \mathbf{A}\mathbf{\Pi}_Q f$  and  $w = T\mathbf{\Pi}_Q f$ . We see that

$$(2.6a) \quad (\boldsymbol{\sigma} - \boldsymbol{\psi}, \boldsymbol{\tau}) + (u - w, \text{rot } \boldsymbol{\tau}) = 0 \quad \forall \boldsymbol{\tau} \in \mathbf{H}_0(\text{rot}, \Omega),$$

$$(2.6b) \quad (\text{rot } (\boldsymbol{\sigma} - \boldsymbol{\psi}), v) = (f - \mathbf{\Pi}_Q f, v) \quad \forall v \in L_0^2(\Omega).$$

Setting  $v = w - u$  in (2.6b) and  $\boldsymbol{\tau} = \boldsymbol{\sigma} - \boldsymbol{\psi}$  in (2.6a), and adding the result yields  $\|\boldsymbol{\sigma} - \boldsymbol{\psi}\|_{L^2(\Omega)}^2 = (f - \mathbf{\Pi}_Q f, w - u)$ . Furthermore, (2.6a) implies  $\mathbf{curl} (u - w) = \boldsymbol{\sigma} - \boldsymbol{\psi}$ . Therefore, there holds

$$\|\boldsymbol{\sigma} - \boldsymbol{\psi}\|_{L^2(\Omega)} \leq \sup_{\phi \in H^1(\Omega) \cap L_0^2(\Omega)} \frac{(f - \mathbf{\Pi}_Q f, \phi)}{\|\mathbf{curl} \phi\|_{L^2(\Omega)}}.$$

However, the properties of the  $L^2$  projection and Assumption 2.3 give us

$$\sup_{\phi \in H^1(\Omega) \cap L_0^2(\Omega)} \frac{(f - \mathbf{\Pi}_Q f, \phi)}{\|\mathbf{curl} \phi\|_{L^2(\Omega)}} = \sup_{\phi \in H^1(\Omega) \cap L_0^2(\Omega)} \frac{(f, \phi - \mathbf{\Pi}_Q \phi)}{\|\mathbf{curl} \phi\|_{L^2(\Omega)}} \leq \omega_1(h)\|f\|_{L^2(\Omega)}.$$

Thus, we have shown

$$\|\mathbf{A}\mathbf{\Pi}_Q f - \mathbf{A}f\|_{L^2(\Omega)} \leq \omega_1(h)\|f\|_{L^2(\Omega)}.$$

Finally, by the Poincare's inequality we have

$$\|T\mathbf{\Pi}_Q f - Tf\|_{L^2(\Omega)} \leq C\|\mathbf{A}\mathbf{\Pi}_Q f - \mathbf{A}f\|_{L^2(\Omega)} \leq C\omega_1(h)\|f\|_{L^2(\Omega)}.$$

□

Next we prove that Assumption 2.3 implies the inf-sup condition for the pair  $(\mathring{\mathbf{V}}_h, \mathring{\mathbf{Q}}_h)$ .

**Lemma 2.6.** Suppose that Assumption 2.3 is satisfied. Then there exists a constant  $C > 0$  such that for every  $u_h \in \mathring{\mathbf{Q}}_h$ , there exists  $\boldsymbol{\tau}_h \in \mathring{\mathbf{V}}_h$  such that  $\text{rot } \boldsymbol{\tau}_h = u_h$  and  $\|\boldsymbol{\tau}_h\|_{L^2(\Omega)} \leq C\|u_h\|_{L^2(\Omega)}$ .

*Proof.* Let  $\boldsymbol{\tau} \in \mathbf{H}_0^1(\Omega)$  with  $\text{rot } \boldsymbol{\tau} = u_h$  such that  $\|\boldsymbol{\tau}\|_{H^1(\Omega)} \leq C\|u_h\|_{L^2(\Omega)}$ . Noting that  $\boldsymbol{\tau} \in \mathring{\mathbf{V}}(Q_h)$ , we define  $\boldsymbol{\tau}_h = \mathbf{\Pi}_V \boldsymbol{\tau}$  so that  $\text{rot } \boldsymbol{\tau}_h = \text{rot } \boldsymbol{\tau} = u_h$ . Moreover,

$$\|\boldsymbol{\tau}_h\|_{L^2(\Omega)} \leq C(\|\boldsymbol{\tau}\|_{H^{1/2+\delta}(\Omega)} + \|\text{rot } \boldsymbol{\tau}\|_{L^2(\Omega)}) \leq C\|\boldsymbol{\tau}\|_{H^1(\Omega)} \leq C\|u_h\|_{L^2(\Omega)}.$$

□

Now we can prove Theorem 2.4.

*Proof of Theorem 2.4.* Let  $f \in L^2(\Omega)$ , and set  $\boldsymbol{\sigma} = \mathbf{A}f$ ,  $u = Tf$  and  $\boldsymbol{\sigma}_h = \mathbf{A}_h f$ ,  $u_h = T_h f$ . Let  $\boldsymbol{\psi} = \mathbf{A}\Pi_Q f$  and  $w = T\Pi_Q f$ .

We first derive an estimate for  $\boldsymbol{\psi} - \boldsymbol{\sigma}_h$ . Using the inclusion  $\text{rot } \mathring{\mathbf{V}}_h \subset \mathring{\mathbf{Q}}_h$ , we see that

$$\begin{aligned} (\Pi_V \boldsymbol{\psi} - \boldsymbol{\sigma}_h, \boldsymbol{\tau}_h) + (\Pi_Q w - u_h, \text{rot } \boldsymbol{\tau}_h) &= (\Pi_V \boldsymbol{\psi} - \boldsymbol{\psi}, \boldsymbol{\tau}_h) \quad \forall \boldsymbol{\tau}_h \in \mathring{\mathbf{V}}_h, \\ (\text{rot } (\Pi_V \boldsymbol{\psi} - \boldsymbol{\sigma}_h), v_h) &= 0 \quad \forall v_h \in \mathring{\mathbf{Q}}_h. \end{aligned}$$

Setting  $\boldsymbol{\tau}_h = \Pi_V \boldsymbol{\psi} - \boldsymbol{\sigma}_h$  and applying the Cauchy–Schwarz inequality yields

$$\|\Pi_V \boldsymbol{\psi} - \boldsymbol{\sigma}_h\|_{L^2(\Omega)} \leq \|\Pi_V \boldsymbol{\psi} - \boldsymbol{\psi}\|_{L^2(\Omega)} \leq \omega_0(h)(\|\boldsymbol{\psi}\|_{H^{1/2+\delta}(\Omega)} + \|\text{rot } \boldsymbol{\psi}\|_{L^2(\Omega)}).$$

If we use Proposition 2.2 we get

$$\|\boldsymbol{\psi}\|_{H^{1/2+\delta}(\Omega)} \leq C(\|\text{div } \boldsymbol{\psi}\|_{L^2(\Omega)} + \|\text{rot } \boldsymbol{\psi}\|_{L^2(\Omega)}) = C\|\text{rot } \boldsymbol{\psi}\|_{L^2(\Omega)} = C\|\Pi_Q f\|_{L^2(\Omega)} \leq C\|f\|_{L^2(\Omega)}.$$

Hence,

$$\|\Pi_V \boldsymbol{\psi} - \boldsymbol{\sigma}_h\|_{L^2(\Omega)} \leq C\omega_0(h)\|f\|_{L^2(\Omega)}.$$

Next, we note that by Lemma 2.5,

$$\|\boldsymbol{\sigma} - \boldsymbol{\psi}\|_{L^2(\Omega)} + \|w - u\|_{L^2(\Omega)} \leq C\omega_1(h)\|f\|_{L^2(\Omega)},$$

and therefore,

$$\begin{aligned} \|(\mathbf{A} - \mathbf{A}_h)f\|_{L^2(\Omega)} &= \|\boldsymbol{\sigma} - \boldsymbol{\sigma}_h\|_{L^2(\Omega)} \\ &\leq \|\boldsymbol{\sigma} - \boldsymbol{\psi}\|_{L^2(\Omega)} + \|\boldsymbol{\sigma}_h - \Pi_V \boldsymbol{\psi}\|_{L^2(\Omega)} + \|\Pi_V \boldsymbol{\psi} - \boldsymbol{\psi}\|_{L^2(\Omega)} \\ &\leq C(\omega_0(h) + \omega_1(h))\|f\|_{L^2(\Omega)}. \end{aligned}$$

Using the inf-sup stability stated in Lemma 2.6, we have

$$\|\Pi_Q w - u_h\|_{L^2(\Omega)} \leq C\|\boldsymbol{\psi} - \boldsymbol{\sigma}_h\|_{L^2(\Omega)} \leq C(\omega_0(h) + \omega_1(h))\|f\|_{L^2(\Omega)}.$$

Hence, we have

$$\begin{aligned} \|w - u_h\|_{L^2(\Omega)} &\leq C(\omega_0(h) + \omega_1(h))\|f\|_{L^2(\Omega)} + \|w - \Pi_Q w\|_{L^2(\Omega)} \\ &\leq C(\omega_0(h) + \omega_1(h))\|f\|_{L^2(\Omega)} + \omega_1(h)\|\text{curl } w\|_{L^2(\Omega)}. \end{aligned}$$

But we have  $\|\text{curl } w\|_{L^2(\Omega)} \leq C\|\Pi_Q f\|_{L^2(\Omega)} \leq C\|f\|_{L^2(\Omega)}$ , and so

$$\|(T - T_h)f\|_{L^2(\Omega)} = \|u - u_h\|_{L^2(\Omega)} \leq C(\omega_0(h) + \omega_1(h))\|f\|_{L^2(\Omega)}.$$

□

### 3. EXAMPLES OF FORTIN OPERATORS

In this section we give examples of finite element pairs satisfying Assumption 2.3, where  $\mathring{\mathbf{V}}_h$  is taken to be a space of continuous, piecewise polynomials, i.e., a Lagrange finite element space. Here we use recent results on divergence-free finite element pairs for the Stokes problem to construct a Fortin projection satisfying (2.5). A common theme of these Stokes pairs is the imposition of mesh conditions for low-polynomial degree finite element spaces; it is well-known that Assumption 2.3 is not satisfied on general simplicial meshes and for low polynomial degree. Before continuing, we introduce some notation.

We denote by  $\mathcal{T}_h$  a shape-regular, simplicial triangulation of  $\Omega$  with  $h_T = \text{diam}(T)$  for all  $T \in \mathcal{T}_h$ , and  $h = \max_{T \in \mathcal{T}_h} h_T$ . Let  $\mathcal{V}_h^I$ ,  $\mathcal{V}_h^B$ ,  $\mathcal{V}_h^C$  denote the sets of interior vertices, boundary vertices, and corner vertices, respectively. Note that the cardinality of  $\mathcal{V}_h^C$  is uniformly bounded due to the shape-regularity of  $\mathcal{T}_h$ . The set of all vertices is  $\mathcal{V}_h = \mathcal{V}_h^I \cup \mathcal{V}_h^B$ . Likewise,  $\mathcal{E}_h^I$  and  $\mathcal{E}_h^B$  are the sets of interior and boundary edges, respectively, and  $\mathcal{E}_h = \mathcal{E}_h^I \cup \mathcal{E}_h^B$ . We denote by  $\mathcal{T}_h(z)$  the patch of triangles that have  $z \in \mathcal{V}_h$  as a vertex. Likewise,  $\mathcal{V}_h^I(T)$  and  $\mathcal{V}_h^B(T)$  are the sets of interior and boundary vertices of  $T \in \mathcal{T}_h$ , and  $\mathcal{E}_h^I(T)$  is the set of interior edges of  $T$ .

For a non-negative integer  $k$  and set  $S \subset \Omega$ , let  $\mathcal{P}_k(S)$  to be the space of piecewise polynomials of degree  $\leq k$  with domain  $S$ . The analogous space of piecewise polynomials with respect to  $\mathcal{T}_h$  is

$$\mathcal{P}_k(\mathcal{T}_h) = \prod_{T \in \mathcal{T}_h} \mathcal{P}_k(T),$$

and the Lagrange finite element space is

$$\mathcal{P}_k^c(\mathcal{T}_h) = \mathcal{P}_k(\mathcal{T}_h) \cap H^1(\Omega).$$

Analogous vector-valued spaces are denoted in boldface, e.g.,  $\mathcal{P}_k(\mathcal{T}_h) = [\mathcal{P}_k(\mathcal{T}_h)]^2$ . Finally, the constant  $C$  denotes a generic constant that is independent of the mesh parameter  $h$  and may take different values at different occurrences.

In the subsequent sections, we will employ a Scott–Zhang type interpolant on the space  $\mathring{\mathbf{V}}$ . We cannot use the Scott–Zhang interpolant directly, as the canonical Scott–Zhang interpolant of a function in  $\mathring{\mathbf{V}}$  might not have zero tangential components at the corners of  $\Omega$ ; hence, we have to modify the Scott–Zhang interpolant at the corners of  $\Omega$ . We give the detailed construction in the appendix but we state the result here.

**Lemma 3.1.** *There exists an interpolant  $\mathbf{I}_h : \mathring{\mathbf{V}} \rightarrow \mathcal{P}_1^c(\mathcal{T}_h) \cap \mathbf{H}_0(\text{rot}, \Omega)$  with the following bound: If  $T \in \mathcal{T}_h$  does not have a corner vertex (i.e.,  $(\mathcal{V}_h^I(T) \cup \mathcal{V}_h^B(T)) \cap \mathcal{V}_h^C = \emptyset$ ), then*

$$(3.1) \quad h_T^{-1/2-\delta} \|\boldsymbol{\tau} - \mathbf{I}_h \boldsymbol{\tau}\|_{L^2(T)} + \|\mathbf{I}_h \boldsymbol{\tau}\|_{H^{1/2+\delta}(T)} \leq C \|\boldsymbol{\tau}\|_{H^{1/2+\delta}(\omega(T))} \quad \forall \boldsymbol{\tau} \in \mathring{\mathbf{V}},$$

where  $\omega(T) = \bigcup_{\substack{T' \in \mathcal{T}_h \\ \bar{T} \cap \bar{T}' \neq \emptyset}} T'$ . Otherwise, if  $T \in \mathcal{T}_h(z)$  for some  $z \in \mathcal{V}_h^C$ , then

$$(3.2) \quad h_T^{-1/2-\delta} \|\boldsymbol{\tau} - \mathbf{I}_h \boldsymbol{\tau}\|_{L^2(T)} + \|\mathbf{I}_h \boldsymbol{\tau}\|_{H^{1/2+\delta}(T)} \leq C \|\boldsymbol{\tau}\|_{H^{1/2+\delta}(\Omega)} \quad \forall \boldsymbol{\tau} \in \mathring{\mathbf{V}}.$$

**3.1. Construction of Fortin Operator on Powell–Sabin Splits.** In this section, we use the recent results given in [16] to construct a Fortin projection into the Lagrange finite element space defined on Powell–Sabin triangulations. For simplicity and readability, we focus on the lowest-order case; however, the arguments easily extend to arbitrary polynomial degree  $k \geq 1$ .

Given the simplicial triangulation of  $\mathcal{T}_h$  of  $\Omega$ , we construct its Powell–Sabin refinement  $\mathcal{T}_h^{\text{ps}}$  as follows [20, 19, 16]: First, adjoin the incenter of each  $T \in \mathcal{T}_h$  to each vertex of  $T$ . Next, the interior points (inceneters) of each adjacent pair of triangles are connected with an edge. For any  $T$  that shares an edge with the boundary of  $\Omega$ , the midpoint of that edge is connected with the incenter of  $T$ . Thus, each  $T \in \mathcal{T}_h$  is split into six triangles; cf. Figure 1.

Let  $\mathcal{S}_h^I(\mathcal{T}_h^{\text{ps}})$  be the points of intersection of the interior edges of  $\mathcal{T}_h$  that adjoin inceneters, let  $\mathcal{S}_h^B(\mathcal{T}_h^{\text{ps}})$  be the intersection points of the boundary edges that adjoin inceneters, and set  $\mathcal{S}_h(\mathcal{T}_h^{\text{ps}}) = \mathcal{S}_h^I(\mathcal{T}_h^{\text{ps}}) \cup \mathcal{S}_h^B(\mathcal{T}_h^{\text{ps}})$ . Note that, by the definition of the Powell–Sabin split, the points in  $\mathcal{S}_h(\mathcal{T}_h^{\text{ps}})$  are the singular vertices in  $\mathcal{T}_h^{\text{ps}}$ , i.e, the vertices that lie on exactly two straight lines. In particular, for a vertex  $z \in \mathcal{S}_h^I(\mathcal{T}_h^{\text{ps}})$  there exists four triangles  $\mathcal{T}_h^{\text{ps}}(z) = \{T_i\}_{i=1}^4 \subset \mathcal{T}_h^{\text{ps}}$  such that  $z$  is a vertex of  $T_i$ . Without loss of generality we assume that these triangles are labeled in a counterclockwise direction. We then define for a scalar function  $v$ ,

$$(3.3) \quad \theta_z(v) := v|_{T_1}(z) - v|_{T_2}(z) + v|_{T_3}(z) - v|_{T_4}(z).$$

We then define the spaces

$$(3.4a) \quad \mathring{\mathbf{V}}_h = \mathcal{P}_1^c(\mathcal{T}_h^{\text{ps}}) \cap \mathbf{H}_0(\text{rot}, \Omega),$$

$$(3.4b) \quad \mathring{\mathbf{Q}}_h = \{v \in \mathcal{P}_0(\mathcal{T}_h^{\text{ps}}) \cap L_0^2(\Omega) : \theta_z(v) = 0 \ \forall z \in \mathcal{S}_h^I(\mathcal{T}_h^{\text{ps}})\}.$$

**Lemma 3.2** ([16]). *Let  $\mathring{\mathbf{V}}_h$  and  $\mathring{\mathbf{Q}}_h$  be defined by (3.4). Then there holds  $\text{rot } \mathring{\mathbf{V}}_h \subset \mathring{\mathbf{Q}}_h$ .*

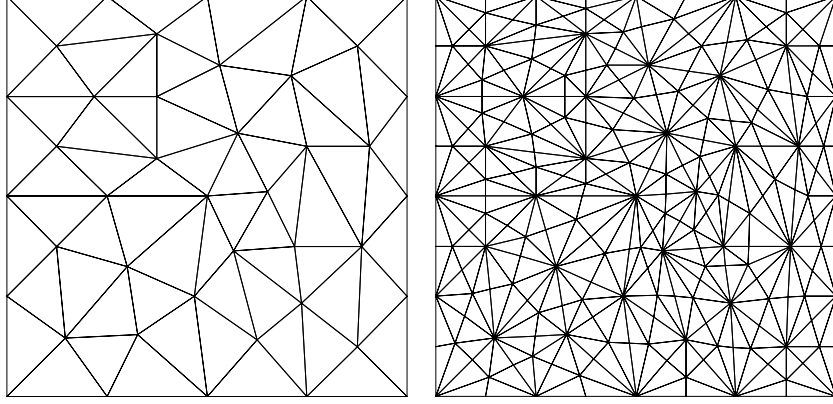


FIGURE 1. A simplicial triangulation of the unit square (left) and the associated Powell–Sabin triangulation (right).

We now extend the results of [16] to construct an appropriate Fortin operator that is well defined for  $\boldsymbol{\tau} \in \mathring{\mathbf{V}}(Q_h)$ . To do so, we require some additional notation.

For an interior singular vertex  $z \in \mathcal{S}_h(\mathcal{T}_h^{\text{ps}})$ , let  $T \in \mathcal{T}_h$  be a triangle in  $\mathcal{T}_h$  such that  $z \in \partial T$ , and let  $\{K_1, K_2\} \subset \mathcal{T}_h^{\text{ps}}$  be the triangles in  $\mathcal{T}_h^{\text{ps}}$  such that  $K_1, K_2 \subset T$  and  $K_1, K_2 \in \mathcal{T}_h^{\text{ps}}(z)$ . Let  $e = \partial K_1 \cap \partial K_2$ , and let  $\mathbf{m}_i$  be the outward unit normal of  $K_i$  perpendicular to  $e$ . We then define the jump of a scalar piecewise smooth function at  $z$  (restricted to  $T$ ) as

$$[[v]]_T(z) = v|_{K_1}(z)\mathbf{m}_1 + v|_{K_2}(z)\mathbf{m}_2.$$

Note that  $[[v]]_T(z)$  is single-valued for all  $v \in \mathring{Q}_h$ . In particular, if  $z$  is an interior singular vertex with  $z \in \partial T_1 \cap \partial T_2$  for some  $T_1, T_2 \in \mathcal{T}_h$ ,  $T_1 \neq T_2$ , then  $[[v]]_{T_1}(z) = [[v]]_{T_2}(z)$  for all  $v \in \mathring{Q}_h$  because  $\theta_z(v) = 0$ . Therefore, we shall omit the subscript and simply write  $[[v]](z)$ .

Next for a triangle  $T \in \mathcal{T}_h$  in the non-refined mesh, we denote by  $T^{\text{ct}}$  the resulting set of three triangles obtained by connecting the barycenter of  $T$  to its vertices, i.e.,  $T^{\text{ct}}$  is the Clough–Tocher refinement of  $T$ . We define the set of (local) piecewise polynomials with respect to this partition as

$$(3.5) \quad \mathcal{P}_k(T^{\text{ct}}) = \prod_{K \in T^{\text{ct}}} \mathcal{P}_k(K).$$

The following lemma provides the degrees of freedom for  $\mathring{\mathbf{V}}_h$  and  $\mathring{Q}_h$  that will be used to construct the Fortin operator. The result essentially follows from [16, Lemma 4.5].

**Lemma 3.3.** *A function  $\boldsymbol{\tau} \in \mathring{\mathbf{V}}_h$  is uniquely defined by the conditions*

$$(3.6a) \quad \boldsymbol{\tau}(z) \quad \forall z \in \mathcal{V}_h^I,$$

$$(3.6b) \quad \boldsymbol{\tau}(z) \cdot \mathbf{n} \quad \forall z \in \mathcal{V}_h^B \setminus \mathcal{V}_h^C,$$

$$(3.6c) \quad \int_e (\boldsymbol{\tau} \cdot \mathbf{t}) \quad \forall e \in \mathcal{E}_h^I,$$

$$(3.6d) \quad [[\text{rot } \boldsymbol{\tau}]](z) \quad \forall z \in \mathcal{S}_h(\mathcal{T}_h^{\text{ps}}),$$

$$(3.6e) \quad \int_T (\text{rot } \boldsymbol{\tau}) r \quad \forall r \in \mathcal{P}_0(T^{\text{ct}}) \cap L_0^2(T), \quad \forall T \in \mathcal{T}_h.$$

Moreover, a function  $v \in \mathring{Q}_h$  is uniquely determined by the values

$$(3.7a) \quad \llbracket v \rrbracket(z) \quad \forall z \in \mathcal{S}_h(\mathcal{T}_h^{\text{ps}}),$$

$$(3.7b) \quad \int_T v r \quad \forall r \in \mathring{\mathcal{P}}_0(T^{\text{ct}}), \quad \forall T \in \mathcal{T}_h.$$

**Theorem 3.4.** *Let  $\mathring{\mathbf{V}}_h$  and  $\mathring{Q}_h$  be defined by (3.4), and let  $\mathring{\mathbf{V}}(Q_h)$  be defined by (2.4). Then there exists a projection  $\mathbf{\Pi}_V : \mathring{\mathbf{V}}(Q_h) \rightarrow \mathring{\mathbf{V}}_h$  such that  $\text{rot } \mathbf{\Pi}_V \mathbf{p} = \text{rot } \mathbf{p}$  for all  $\mathbf{p} \in \mathring{\mathbf{V}}(Q_h)$ . Moreover,*

$$\|\boldsymbol{\tau} - \mathbf{\Pi}_V \boldsymbol{\tau}\|_{L^2(\Omega)} \leq C(h^{1/2+\delta} \|\boldsymbol{\tau}\|_{H^{1/2+\delta}(\Omega)} + h \|\text{rot } \boldsymbol{\tau}\|_{L^2(\Omega)}).$$

*Proof.* Fix  $\boldsymbol{\tau} \in \mathring{\mathbf{V}}(Q_h)$ , and let  $\mathbf{I}_h \boldsymbol{\tau} \in \mathcal{P}_1^c(\mathcal{T}_h) \cap \mathbf{H}_0(\text{rot}, \Omega) \subset \mathring{\mathbf{V}}_h$  be the modified Scott–Zhang interpolant of  $\boldsymbol{\tau}$  established in Lemma 3.1. We then construct  $\mathbf{\Pi}_V \boldsymbol{\tau}$  via the conditions

$$(3.8a) \quad (\mathbf{\Pi}_V \boldsymbol{\tau})(z) = (\mathbf{I}_h \boldsymbol{\tau})(z) \quad \forall z \in \mathcal{V}_h^I,$$

$$(3.8b) \quad (\mathbf{\Pi}_V \boldsymbol{\tau})(z) \cdot \mathbf{n} = (\mathbf{I}_h \boldsymbol{\tau})(z) \cdot \mathbf{n} \quad \forall z \in \mathcal{V}_h^B \setminus \mathcal{V}_h^C,$$

$$(3.8c) \quad \int_e (\mathbf{\Pi}_V \boldsymbol{\tau}) \cdot \mathbf{t} = \int_e \boldsymbol{\tau} \cdot \mathbf{t} \quad \forall e \in \mathcal{E}_h^I,$$

$$(3.8d) \quad \llbracket \text{rot } \mathbf{\Pi}_V \boldsymbol{\tau} \rrbracket(z) = \llbracket \text{rot } \boldsymbol{\tau} \rrbracket(z) \quad \forall z \in \mathcal{S}_h(\mathcal{T}_h^{\text{ps}}),$$

$$(3.8e) \quad \int_T (\text{rot } \mathbf{\Pi}_V \boldsymbol{\tau}) q = \int_T (\text{rot } \boldsymbol{\tau}) q \quad \forall r \in \mathring{\mathcal{P}}_0(T^{\text{ct}}), \quad \forall T \in \mathcal{T}_h.$$

The arguments given in [16] show that  $\text{rot } \mathbf{\Pi}_V \boldsymbol{\tau} = \text{rot } \boldsymbol{\tau}$ ,

By scaling, there holds for each  $\boldsymbol{\sigma}_h \in \mathring{\mathbf{V}}_h$  and on each  $T \in \mathcal{T}_h$ ,

$$\begin{aligned} \|\boldsymbol{\sigma}_h\|_{L^2(T)}^2 &\leq C \left[ h_T^2 \left( \sum_{z \in \mathcal{V}_h^I(T)} |\boldsymbol{\sigma}_h(z)|^2 + \sum_{z \in \mathcal{V}_h^B(T) \setminus \mathcal{V}_h^C(T)} |\boldsymbol{\sigma}_h(z) \cdot \mathbf{n}|^2 \right) \right. \\ &\quad + \sum_{e \in \mathcal{E}_h^I(T)} \left| \int_e \boldsymbol{\sigma}_h \cdot \mathbf{t} \right|^2 + h_T^2 \sup_{\substack{r \in \mathcal{P}_0(T^{\text{ct}}) \\ \|r\|_{L^2(T)}=1}} \left| \int_T (\text{rot } \boldsymbol{\sigma}_h) r \right|^2 \\ &\quad \left. + h_T^4 \sum_{z \in \mathcal{S}_h(T)} |\llbracket \text{rot } \boldsymbol{\sigma}_h \rrbracket(z)|^2 \right]. \end{aligned}$$

Now set  $\boldsymbol{\sigma}_h = \mathbf{\Pi}_V \boldsymbol{\tau} - \mathbf{I}_h \boldsymbol{\tau}$ . Using the above estimate and (3.8) then yields

$$(3.9) \quad \begin{aligned} \|\mathbf{\Pi}_V \boldsymbol{\tau} - \mathbf{I}_h \boldsymbol{\tau}\|_{L^2(T)}^2 &\leq C \left[ \left| \int_{\partial T} (\boldsymbol{\tau} - \mathbf{I}_h \boldsymbol{\tau}) \cdot \mathbf{t} \right|^2 + h_T^2 \sup_{\substack{r \in \mathcal{P}_0(T^{\text{ct}}) \\ \|r\|_{L^2(T)}=1}} \left| \int_T (\text{rot } (\boldsymbol{\tau} - \mathbf{I}_h \boldsymbol{\tau})) r \right|^2 \right. \\ &\quad \left. + h_T^4 \sum_{z \in \mathcal{S}_h(T)} |\llbracket \text{rot } (\boldsymbol{\tau} - \mathbf{I}_h \boldsymbol{\tau}) \rrbracket(z)|^2 \right]. \end{aligned}$$

Because  $\text{rot } (\boldsymbol{\tau} - \mathbf{I}_h \boldsymbol{\tau}) \in \mathring{Q}_h$ , we use the degrees of freedom (3.7) and a scaling argument to conclude that

$$(3.10) \quad \begin{aligned} \sup_{\substack{r \in \mathcal{P}_0(T^{\text{ct}}) \\ \|r\|_{L^2(T)}=1}} \left| \int_T (\text{rot } (\boldsymbol{\tau} - \mathbf{I}_h \boldsymbol{\tau})) r \right|^2 + h_T^2 \sum_{z \in \mathcal{M}_h(T) \cup \mathcal{M}_h^B(T)} |\llbracket \text{rot } (\boldsymbol{\tau} - \mathbf{I}_h \boldsymbol{\tau}) \rrbracket(z)|^2 \\ \leq C \|\text{rot } (\boldsymbol{\tau} - \mathbf{I}_h \boldsymbol{\tau})\|_{L^2(T)}^2. \end{aligned}$$

We then use an inverse estimate to get

$$(3.11) \quad \begin{aligned} \|\text{rot } (\boldsymbol{\tau} - \mathbf{I}_h \boldsymbol{\tau})\|_{L^2(T)}^2 &\leq C [\|\text{rot } \boldsymbol{\tau}\|_{L^2(T)}^2 + \|\nabla \mathbf{I}_h \boldsymbol{\tau}\|_{L^2(T)}^2] \\ &\leq C [\|\text{rot } \boldsymbol{\tau}\|_{L^2(T)}^2 + h_T^{-1+2\delta} \|\mathbf{I}_h \boldsymbol{\tau}\|_{H^{1/2+\delta}(T)}^2]. \end{aligned}$$



Applying the estimates (3.10)–(3.11) to (3.9), we obtain

$$\begin{aligned} \|\Pi_V \boldsymbol{\tau} - \mathbf{I}_h \boldsymbol{\tau}\|_{L^2(T)}^2 &\leq C \left[ \left| \int_{\partial T} (\boldsymbol{\tau} - \mathbf{I}_h \boldsymbol{\tau}) \cdot \mathbf{t} \right|^2 + h_T^2 (\|\operatorname{rot} \boldsymbol{\tau}\|_{L^2(T)}^2 + h_T^{-1+2\delta} \|\mathbf{I}_h \boldsymbol{\tau}\|_{H^{1/2+\delta}(\omega(T))}^2) \right] \\ &\leq C [h_T \|\boldsymbol{\tau} - \mathbf{I}_h \boldsymbol{\tau}\|_{L^2(\partial T)}^2 + h_T^{1+2\delta} \|\mathbf{I}_h \boldsymbol{\tau}\|_{H^{1/2+\delta}(T)}^2 + h_T^2 \|\operatorname{rot} \boldsymbol{\tau}\|_{L^2(T)}^2]. \end{aligned}$$

We then apply (3.1)–(3.2) and sum over  $T \in \mathcal{T}_h$  to obtain

$$\|\Pi_V \boldsymbol{\tau} - \mathbf{I}_h \boldsymbol{\tau}\|_{L^2(\Omega)}^2 \leq C [h^{1/2+\delta} \|\boldsymbol{\tau}\|_{H^{1/2+\delta}(\Omega)}^2 + h \|\operatorname{rot} \boldsymbol{\tau}\|_{L^2(\Omega)}^2].$$

Therefore

$$\|\boldsymbol{\tau} - \Pi_V \boldsymbol{\tau}\|_{L^2(\Omega)} \leq \|\boldsymbol{\tau} - \mathbf{I}_h \boldsymbol{\tau}\|_{L^2(\Omega)} + \|\Pi_V \boldsymbol{\tau} - \mathbf{I}_h \boldsymbol{\tau}\|_{L^2(\Omega)} \leq C [h^{1/2+\delta} \|\boldsymbol{\tau}\|_{H^{1/2+\delta}(\Omega)} + h \|\operatorname{rot} \boldsymbol{\tau}\|_{L^2(\Omega)}].$$

□

**3.2. Construction of Fortin Operator on Clough–Tocher Splits.** The Clough–Tocher refinement of  $\mathcal{T}_h$  is obtained by connecting the barycenter of each  $T \in \mathcal{T}_h$  with its vertices; thus, each triangle is split into three triangles. In this section, we show that there exists a Fortin projection mapping onto the Lagrange finite element space satisfying Assumption 2.3. This result holds for all polynomial degrees  $k \geq 2$  but, for simplicity, we only consider the lowest order case  $k = 2$ .

Let  $\mathcal{T}_h^{\text{ct}}$  be the resulting Clough–Tocher refinement of  $\mathcal{T}_h$ , and define the spaces

$$(3.12a) \quad \mathring{\mathbf{V}}_h = \mathcal{P}_2^c(\mathcal{T}_h^{\text{ct}}) \cap \mathbf{H}_0(\operatorname{rot}, \Omega),$$

$$(3.12b) \quad \mathring{Q}_h = L_0^2(\Omega) \cap \mathcal{P}_1(\mathcal{T}_h^{\text{ct}}).$$

It is well-known that  $\operatorname{rot} \mathring{\mathbf{V}}_h \subset \mathring{Q}_h$  [15].

Below we modify the results in [15] to build a Fortin projection that is well-defined on  $\mathbf{H}^{1/2+\delta}(\Omega)$  and has optimal order convergence properties in  $L^2(\Omega)$ . To this end, we first provide a useful set of degrees of freedom for  $\mathring{\mathbf{V}}_h$  [15].

**Lemma 3.5.** *A function  $\boldsymbol{\tau} \in \mathring{\mathbf{V}}_h$  is uniquely determined by the values*

$$(3.13) \quad \boldsymbol{\tau}(z) \quad \forall z \in \mathcal{V}_h^I,$$

$$(3.14) \quad \boldsymbol{\tau}(z) \cdot \mathbf{n} \quad \forall z \in \mathcal{V}_h^B \setminus \mathcal{V}_h^C,$$

$$(3.15) \quad \int_e \boldsymbol{\tau} \quad \forall e \in \mathcal{E}_h^I,$$

$$(3.16) \quad \int_e \boldsymbol{\tau} \cdot \mathbf{n} \quad \forall e \in \mathcal{E}_h^B,$$

$$(3.17) \quad \int_T (\operatorname{rot} \boldsymbol{\tau}) r \quad \forall r \in \mathcal{P}_1(T^{\text{ct}}) \cap L_0^2(T), \quad \forall T \in \mathcal{T}_h,$$

where  $\mathcal{P}_1(T^{\text{ct}})$  is defined by (3.5).

**Theorem 3.6.** *Let  $\mathring{\mathbf{V}}_h$  and  $\mathring{Q}_h$  be defined by (3.12), and let  $\Pi_Q$  be the  $L^2$  projection onto  $\mathring{Q}_h$ . Then there exists a projection  $\Pi_V : \mathring{\mathbf{V}}(Q_h) \rightarrow \mathring{\mathbf{V}}_h$ , such that  $\operatorname{rot} \Pi_V \boldsymbol{\tau} = \Pi_Q(\operatorname{rot} \boldsymbol{\tau})$ . Moreover,*

$$\|\boldsymbol{\tau} - \Pi_V \boldsymbol{\tau}\|_{L^2(\Omega)} \leq C (h^{1/2+\delta} \|\boldsymbol{\tau}\|_{H^{1/2+\delta}(\Omega)} + h \|\operatorname{rot} \boldsymbol{\tau}\|_{L^2(\Omega)}).$$

*Proof.* Define  $\Pi_V$  uniquely by the conditions

$$(3.18a) \quad (\Pi_V \boldsymbol{\tau})(z) = (\mathbf{I}_h \boldsymbol{\tau})(z) \quad \forall z \in \mathcal{V}_h^I,$$

$$(3.18b) \quad (\Pi_V \boldsymbol{\tau})(z) \cdot \mathbf{n} = (\mathbf{I}_h \boldsymbol{\tau})(z) \cdot \mathbf{n} \quad \forall z \in \mathcal{V}_h^B \setminus \mathcal{V}_h^C,$$

$$(3.18c) \quad \int_e (\Pi_V \boldsymbol{\tau}) = \int_e \boldsymbol{\tau} \quad \forall e \in \mathcal{E}_h^I,$$

$$(3.18d) \quad \int_e (\Pi_V \boldsymbol{\tau} \cdot \mathbf{n}) = \int_e \boldsymbol{\tau} \cdot \mathbf{n} \quad \forall e \in \mathcal{E}_h^B,$$

$$(3.18e) \quad \int_T (\text{rot } \Pi_V \boldsymbol{\tau}) r = \int_T (\text{rot } \boldsymbol{\tau}) r \quad \forall r \in \mathcal{P}_1(T^{\text{ct}}) \cap L_0^2(T), \quad \forall T \in \mathcal{T}_h.$$

The arguments given in [15] show that  $\text{rot } \Pi_V \boldsymbol{\tau} = \Pi_Q \text{rot } \boldsymbol{\tau}$ . The same scaling arguments given in Theorem 3.4 show that  $\|\boldsymbol{\tau} - \Pi_V \boldsymbol{\tau}\|_{L^2(\Omega)} \leq C(h^{1/2+\delta} \|\boldsymbol{\tau}\|_{H^{1/2+\delta}(\Omega)} + h \|\text{rot } \boldsymbol{\tau}\|_{L^2(\Omega)})$ .  $\square$

**3.3. Construction of Fortin Operator on General Triangulations.** In this section, we construct a Fortin operator for the original Scott–Vogelius pair developed in [22]. This pair essentially takes the space  $\dot{\mathbf{V}}_h$  to be the Lagrange space of degree  $k \geq 4$ , and  $\dot{\mathbf{Q}}_h$  to be the space of piecewise polynomials of degree  $(k-1)$ . As pointed out in [22] the exact definition of these spaces and their stability is mesh-dependent and depends on the presence of singular or “nearly singular” vertices.

Recall that a singular vertex is a vertex in  $\mathcal{T}_h$  that lies on exactly two straight lines. To make this precise, for a vertex  $z \in \mathcal{V}_h$ , we enumerate the triangles that have  $z$  as a vertex as  $\mathcal{T}_h(z) = \{T_1, T_2, \dots, T_N\}$ . If  $z$  is a boundary vertex then we enumerate the triangles such that  $T_1$  and  $T_N$  have a boundary edge. Moreover, we enumerate them so that  $T_j, T_{j+1}$  share an edge for  $j = 1, \dots, N-1$  and  $T_N$  and  $T_1$  share an edge in the case  $z$  is an interior vertex. Let  $\theta_j$  denote the angle between the edges of  $T_j$  originating from  $z$ . We define

$$(3.19) \quad \Theta(z) = \begin{cases} \max\{|\sin(\theta_1 + \theta_2)|, \dots, |\sin(\theta_{N-1} + \theta_N)|, |\sin(\theta_N + \theta_1)|\} & \text{if } z \in \mathcal{V}_h^I \\ \max\{|\sin(\theta_1 + \theta_2)|, \dots, |\sin(\theta_{N-1} + \theta_N)|\} & \text{if } z \in \mathcal{V}_h^B \text{ and } N \geq 2, \\ 0 & \text{if } z \in \mathcal{V}_h^B \text{ and } N = 1. \end{cases}$$

**Definition 3.7.** A vertex  $z \in \mathcal{V}_h$  is a singular vertex if  $\Theta(z) = 0$ . It is non-singular if  $\Theta(z) > 0$ .

We denote all the singular vertices by

$$\mathcal{S}_h = \{z \in \mathcal{V}_h : \Theta(z) = 0\}.$$

We further let  $\mathcal{S}_h^I$  denote the set of interior singular vertices,  $\mathcal{S}_h^B$  the set of boundary singular vertices, and  $\mathcal{S}_h^C$  the set of corner singular vertices. Equivalently,

$$\begin{aligned} \mathcal{S}_h^I &= \{z \in \mathcal{S}_h : \#\mathcal{T}_h(z) = 4\}, \\ \mathcal{S}_h^B &= \{z \in \mathcal{S}_h : \#\mathcal{T}_h(z) \in \{1, 2\}\}, \\ \mathcal{S}_h^C &= \{z \in \mathcal{S}_h : \#\mathcal{T}_h(z) = 1\}. \end{aligned}$$

**Definition 3.8.** We set

$$(3.20) \quad \Theta_{\min} := \min_{z \in \mathcal{V}_h \setminus \mathcal{S}_h} \Theta(z).$$

For a non-negative integer  $k$ , we define the spaces

$$(3.21a) \quad \dot{\mathbf{V}}_h = \mathcal{P}_k^c(\mathcal{T}_h) \cap \mathbf{H}_0(\text{rot}, \Omega),$$

$$(3.21b) \quad \dot{\mathbf{Q}}_h = \{v \in L_0^2(\Omega) \cap \mathcal{P}_{k-1}(\mathcal{T}_h) : \theta_z(v) = 0 \quad \forall z \in \mathcal{S}_h^I, \quad v(z) = 0 \quad \forall z \in \mathcal{S}_h^C\},$$

where we recall that  $\theta_z(v)$  is defined by (3.3).

First we note that the rot operator maps  $\dot{\mathbf{V}}_h$  into  $\dot{\mathbf{Q}}_h$  [22].

**Lemma 3.9.** *There holds  $\text{rot } \boldsymbol{\tau} \in \dot{\mathbf{Q}}_h$  for all  $\boldsymbol{\tau} \in \dot{\mathbf{V}}_h$ .*

Let  $\mathbf{I}_h$  be Scott–Zhang interpolant onto  $\mathcal{P}_1^c(\mathcal{T}_h) \cap \mathbf{H}_0(\text{rot}; \Omega) \subset \mathring{\mathbf{V}}_h$ . Then define  $\mathbf{I}_1 : \mathbf{H}^{1/2+\delta}(\Omega) \rightarrow \mathring{\mathbf{V}}_h$  as follows

$$\begin{aligned} \mathbf{I}_1 \boldsymbol{\tau}(z) &= \mathbf{I}_h \boldsymbol{\tau}(z) \quad \forall z \in \mathcal{V}_h, \\ \int_e \mathbf{I}_1 \boldsymbol{\tau} \cdot \boldsymbol{\psi} &= \int_e \boldsymbol{\tau} \cdot \boldsymbol{\psi} \quad \text{for all } \boldsymbol{\psi} \in \mathcal{P}_{k-2}(e), \forall e \in \mathcal{E}_h, \\ \int_T \mathbf{I}_1 \boldsymbol{\tau} \cdot \boldsymbol{\psi} &= \int_T \boldsymbol{\tau} \cdot \boldsymbol{\psi} \quad \text{for all } \boldsymbol{\psi} \in \mathcal{P}_{k-3}(T), \forall T \in \mathcal{T}_h. \end{aligned}$$

Standard arguments yield the following result.

**Lemma 3.10.** *There holds for all  $\boldsymbol{\tau} \in \mathbf{H}^{1/2+\delta}(\Omega)$*

$$(3.22) \quad \|\boldsymbol{\tau} - \mathbf{I}_1 \boldsymbol{\tau}\|_{L^2(\Omega)} \leq Ch^{1/2+\delta} \|\boldsymbol{\tau}\|_{\mathbf{H}^{1/2+\delta}(\Omega)}.$$

and

$$(3.23) \quad \|\text{rot}(\mathbf{I}_1 \boldsymbol{\tau})\|_{L^2(\Omega)} \leq h^{-1/2+\delta} \|\boldsymbol{\tau}\|_{\mathbf{H}^{1/2+\delta}(\Omega)}.$$

Moreover, for  $k \geq 2$ ,

$$(3.24) \quad \int_T \text{rot} \mathbf{I}_1 \boldsymbol{\tau} = \int_T \text{rot} \boldsymbol{\tau} \quad \forall T \in \mathcal{T}_h.$$

The following result follows from [17, Lemma 6].

**Lemma 3.11.** *Suppose that  $k \geq 4$ . Then there exists an injective linear operator  $\mathbf{J}_1 : \mathring{\mathbf{Q}}_h \rightarrow \mathring{\mathbf{V}}_h$  such that*

$$(3.25a) \quad \text{rot}(\mathbf{J}_1 v)(z) = v(z) \quad \forall z \in \mathcal{V}_h,$$

$$(3.25b) \quad \int_T \text{rot}(\mathbf{J}_1 v) dx = 0 \quad \forall T \in \mathcal{T}_h,$$

$$(3.25c) \quad \|\mathbf{J}_1 v\|_{L^2(\Omega)} + h \|\nabla \mathbf{J}_1 v\|_{L^2(\Omega)} \leq Ch \left( \frac{1}{\Theta_{\min}} + 1 \right) \|v\|_{L^2(\Omega)}.$$

The following result follows from [22, 14, 17].

**Lemma 3.12.** *Define*

$$\mathring{\mathbf{Q}}_h = \{v \in \mathring{\mathbf{Q}}_h : \int_T v = 0 \ \forall T \in \mathcal{T}_h, \text{ and } v(z) = 0 \ \forall z \in \mathcal{V}_h\}.$$

Then there exists an injective operator  $\mathbf{J}_2 : \mathring{\mathbf{Q}}_h \rightarrow \mathring{\mathbf{V}}_h$  such that

$$\begin{aligned} \text{rot}(\mathbf{J}_2 v) &= v, \\ \|\mathbf{J}_2 v\|_{L^2(\Omega)} + h \|\nabla \mathbf{J}_2 v\|_{L^2(\Omega)} &\leq Ch \|v\|_{L^2(\Omega)}. \end{aligned}$$

**Theorem 3.13.** *Let  $\mathring{\mathbf{V}}_h$  and  $\mathring{\mathbf{Q}}_h$  be defined by (3.21) with  $k \geq 4$ . Then there exists a projection  $\mathbf{\Pi}_V : \mathring{\mathbf{V}}(Q_h) \rightarrow \mathring{\mathbf{V}}_h$  such that*

$$\text{rot}(\mathbf{\Pi}_V \boldsymbol{\tau}) = \text{rot} \boldsymbol{\tau}$$

with the following bound

$$\|\boldsymbol{\tau} - \mathbf{\Pi}_V \boldsymbol{\tau}\|_{L^2(\Omega)} \leq C(1 + \Theta_{\min}^{-1}) h^{1/2+\delta} \|\boldsymbol{\tau}\|_{\mathbf{H}^{1/2+\delta}(\Omega)}.$$

*Proof.* Define:

$$\mathbf{\Pi}_V \boldsymbol{\tau} = \mathbf{I}_1 \boldsymbol{\tau} + \mathbf{J}_1 v_1 + \mathbf{J}_2 v_2 \in \mathring{\mathbf{V}}_h,$$

where

$$v_1 = \text{rot}(\boldsymbol{\tau} - \mathbf{I}_1 \boldsymbol{\tau}) \in \mathring{\mathbf{Q}}_h, \quad v_2 = v_1 - \text{rot}(\mathbf{J}_1 v_1) \in \mathring{\mathbf{Q}}_h.$$

By Lemma 3.11 and the definition of  $v_2$ , we see that

$$v_2(z) = 0 \quad \forall z \in \mathcal{V}_h,$$

and

$$\int_T v_2 = \int_T (v_1 - \operatorname{rot}(\mathbf{J}_1 v_1)) = \int_T v_1 = \int_T \operatorname{rot}(\boldsymbol{\tau} - \mathbf{I}_1 \boldsymbol{\tau}) = 0,$$

by Lemma 3.10. Therefore  $v_2 \in \mathring{Q}_h$ , and so  $\mathbf{J}_2 v_2$  is well-defined (cf. Lemma 3.12).

We then use Lemma 3.12 to get

$$\begin{aligned} \operatorname{rot}(\boldsymbol{\Pi}_V \boldsymbol{\tau}) &= \operatorname{rot}(\mathbf{I}_1 \boldsymbol{\tau}) + \operatorname{rot}(\mathbf{J}_1 v_1) + \operatorname{rot}(\mathbf{J}_2 v_2) \\ &= \operatorname{rot}(\mathbf{I}_1 \boldsymbol{\tau}) + \operatorname{rot}(\mathbf{J}_1 v_1) + v_2 \\ &= \operatorname{rot}(\mathbf{I}_1 \boldsymbol{\tau}) + \operatorname{rot}(\mathbf{J}_1 v_1) + (v_1 - \operatorname{rot}(\mathbf{J}_1 v_1)) \\ &= \operatorname{rot}(\mathbf{I}_1 \boldsymbol{\tau}) + v_1 \\ &= \operatorname{rot}(\mathbf{I}_1 \boldsymbol{\tau}) + \operatorname{rot}(\boldsymbol{\tau} - \mathbf{I}_1 \boldsymbol{\tau}) \\ &= \operatorname{rot} \boldsymbol{\tau}. \end{aligned}$$

Now we note that, by (3.23),

$$\begin{aligned} \|\operatorname{rot}(\boldsymbol{\tau} - \mathbf{I}_1 \boldsymbol{\tau})\|_{L^2(\Omega)} &\leq \|\operatorname{rot} \boldsymbol{\tau}\|_{L^2(\Omega)} + \|\operatorname{rot}(\mathbf{I}_1 \boldsymbol{\tau})\|_{L^2(\Omega)} \\ (3.26) \quad &\leq \|\operatorname{rot} \boldsymbol{\tau}\|_{L^2(\Omega)} + h^{-1/2+\delta} \|\boldsymbol{\tau}\|_{H^{1/2+\delta}(\Omega)}. \end{aligned}$$

Next, by Lemma 3.11 and (3.26) we obtain

$$\begin{aligned} (3.27) \quad \|\mathbf{J}_1 v_1\|_{L^2(\Omega)} &\leq Ch \left( \frac{1}{\Theta_{\min}} + 1 \right) \|v_1\|_{L^2(\Omega)} \\ &\leq Ch \left( \frac{1}{\Theta_{\min}} + 1 \right) \|\operatorname{rot}(\boldsymbol{\tau} - \mathbf{I}_1 \boldsymbol{\tau})\|_{L^2(\Omega)} \\ &\leq C \left( \frac{1}{\Theta_{\min}} + 1 \right) (h \|\operatorname{rot} \boldsymbol{\tau}\|_{L^2(\Omega)} + h^{1/2+\delta} \|\boldsymbol{\tau}\|_{H^{1/2+\delta}(\Omega)}). \end{aligned}$$

Likewise, we use Lemmas 3.12 and (3.26) to obtain

$$\begin{aligned} (3.28) \quad \|\mathbf{J}_2 v_2\|_{L^2(\Omega)} &\leq Ch \|v_2\|_{L^2(\Omega)} \\ &\leq Ch (\|v_1\|_{L^2(\Omega)} + \|\operatorname{rot}(\mathbf{J}_1 v_1)\|_{L^2(\Omega)}) \\ &\leq C (h \|\operatorname{rot}(\boldsymbol{\tau} - \mathbf{I}_1 \boldsymbol{\tau})\|_{L^2(\Omega)} + \|\mathbf{J}_1 v_1\|_{L^2(\Omega)}) \\ &\leq C \left( \frac{1}{\Theta_{\min}} + 1 \right) (h \|\operatorname{rot} \boldsymbol{\tau}\|_{L^2(\Omega)} + h^{1/2+\delta} \|\boldsymbol{\tau}\|_{H^{1/2+\delta}(\Omega)}). \end{aligned}$$

We then use the triangle inequality, Lemma 3.10, (3.27), and (3.28) to obtain the  $L^2$  error estimate:

$$\begin{aligned} \|\boldsymbol{\tau} - \boldsymbol{\Pi}_V \boldsymbol{\tau}\|_{L^2(\Omega)} &\leq \|\boldsymbol{\tau} - \mathbf{I}_1 \boldsymbol{\tau}\|_{L^2(\Omega)} + \|\mathbf{J}_1 v_1\|_{L^2(\Omega)} + \|\mathbf{J}_2 v_2\|_{L^2(\Omega)} \\ &\leq C \left( \frac{1}{\Theta_{\min}} + 1 \right) h^{1/2+\delta} \|\boldsymbol{\tau}\|_{H^{1/2+\delta}(\Omega)}. \end{aligned}$$

Finally, if  $\boldsymbol{\tau} \in \mathring{\mathbf{V}}_h$ , then  $\mathbf{I}_1 \boldsymbol{\tau} = \boldsymbol{\tau}$  and so  $v_1 = 0$ . It then follows that  $\mathbf{J}_1 v_1 = 0$ , and  $\mathbf{J}_2 v_2 = -\mathbf{J}_2(\operatorname{rot}(\mathbf{J}_1 v_1)) = 0$ . Therefore  $\boldsymbol{\Pi}_V \boldsymbol{\tau} = \mathbf{I}_1 \boldsymbol{\tau} = \boldsymbol{\tau}$ , i.e.,  $\boldsymbol{\Pi}_V$  is a projection.  $\square$

#### 4. NUMERICAL EXPERIMENTS

In this section we confirm the theoretical results with some numerical experiments on a variety of meshes and finite element spaces. All the numerical experiments were performed using **Fenics** [1]. In all tests, we take the domain to be the unit square  $\Omega = (0, 1)^2$ . The exact eigenvectors, corresponding to non-zero eigenvalues, are  $\mathbf{u}^{(n,m)}(x, y) := \operatorname{curl} p^{(n,m)}$  where  $p^{(n,m)} := \cos(\pi n x) \cos(\pi m y)$ , with eigenvalues  $\lambda^{(n,m)} := \pi^2(n^2 + m^2)$  for  $n, m \in \mathbb{N} \cup \{0\}$  and  $nm \neq 0$ . In the following we relabel the non-zero eigenvalues  $\lambda^{(i)}$  in non-decreasing order:  $0 < \lambda^{(1)} \leq \lambda^{(2)} \leq \lambda^{(3)} \leq \dots$

**4.1. Linear Lagrange elements on Powell–Sabin triangulations.** In these series of tests, we compute the finite element method (1.2) using piecewise linear Lagrange elements defined on Powell–Sabin triangulations. We create a sequence of generic Delaunay triangulations  $\mathcal{T}_h$  with mesh size  $h_j = 2^{-j}$  for  $j = 3, 4, 5, 6$ , and perform the refinement algorithm described in Section 3.1 to obtain a Powell–Sabin triangulation  $\mathcal{T}_h^{\text{ps}}$  for each mesh parameter.

In Table 1, we show the first ten non-zero approximate eigenvalues and errors using method (1.2) defined on  $\mathcal{T}_h^{\text{ps}}$  for fixed  $h = 1/32$ . In Table 2, we list the rate of convergence of the first eigenvalue with respect to  $h$ . The tables show an absence of spurious eigenvalues which agrees with the theoretical results, Theorems 2.4 and 3.4. In addition, we observe an asymptotic quadratic rate of convergence for the computed eigenvalue.

$i$	$\lambda_h^{(i)}$	$ \lambda^{(i)} - \lambda_h^{(i)} $
1	9.872556542826	2.952141736802360E-3
2	9.872647617226	3.043216136799032E-3
3	19.75126057536	1.205177318315975E-2
4	39.52514303832	4.672543396706175E-2
5	39.52979992791	5.138232355238159E-2
6	49.42354393173	7.552192628650545E-2
7	49.43033089264	8.230888719544538E-2
8	79.15457141878	1.977362100693938E-1
9	89.06160447391	2.351648641029839E-1
10	89.07453060702	2.480909972125715E-1

TABLE 1. Approximate eigenvalues of (1.2) using the piecewise linear Lagrange finite element space on a Powell–Sabin triangulation. The mesh parameter is  $h = 2^{-5}$ .

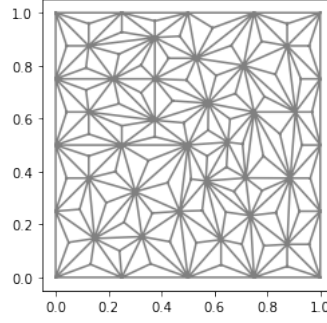
$h$	$ \lambda^{(1)} - \lambda_h^{(1)} $	rate
$2^{-3}$	1.084194558097806E-1	
$2^{-4}$	3.835460507298371E-2	1.8228
$2^{-5}$	2.952141736802360E-3	1.8768
$2^{-6}$	7.488421347368046E-4	1.9790

TABLE 2. The rate of convergence with respect to  $h$  of first non-zero eigenvalue using for Powell–Sabin split and the linear Lagrange finite element space.

**4.2. Quadratic Lagrange elements on Clough–Tocher triangulations.** In this section, we compute the finite element method (1.2) using quadratic Lagrange elements defined on Clough–Tocher triangulations (cf. Section 3.2). As before, we create a sequence of meshes  $\mathcal{T}_h$  with  $h_j = 2^{-j}$  ( $j = 3, 4, 5, 6$ ), and construct the Clough–Tocher refinement  $\mathcal{T}_h^{\text{ct}}$  by connecting the vertices of each triangle in  $\mathcal{T}_h$  with its barycenter; see Figure 2.

In Table 3 we report the first computed ten non-zero approximate eigenvalues using method (1.2). As predicted by Theorems 2.4 and 3.6, the results show accurate approximations with no spurious eigenvalues. In Table 4 we list the rate of convergence to the first eigenvalue for different values of  $h$ . The table clearly shows an asymptotic quartic rate of convergence:  $|\lambda^{(1)} - \lambda_h^{(1)}| = \mathcal{O}(h^4)$ .

**4.3. Quartic Lagrange elements on criss-cross triangulations.** In this section we compute the finite element method (1.2) using fourth degree Lagrange elements on several types of triangulations. Theorems 2.4 and 3.13 indicate that this scheme leads to convergent eigenvalue approximations as  $h \rightarrow 0$  if the quantity  $\Theta_{\min}$  is uniformly bounded from below. We recall that the quantity  $\Theta_{\min}$  gives

FIGURE 2. A Clough-Tocher triangulation with  $h = 2^{-3}$ .

$i$	$\lambda_h^{(i)}$	$ \lambda^{(i)} - \lambda_h^{(i)} $
1	9.869606458779	2.057689641788E-6
2	9.869606625899	2.224809986018E-6
3	19.73922733515	1.853298115861E-5
4	39.47853970719	1.221028349079E-4
5	39.47855143244	1.338280896661E-4
6	49.34827341503	2.514095869017E-4
7	49.34829772352	2.757180775106E-4
8	78.95794423573	1.109027018615E-3
9	88.82788915584	1.449546038714E-3
10	88.82798471962	1.545109821734E-3

TABLE 3. Approximate eigenvalues using quadratic Lagrange elements on a Clough-Tocher triangulation with  $h = 2^{-5}$ .

$h$	$ \lambda^{(1)} - \lambda_h^{(1)} $	rate
$2^{-3}$	2.98012061403341E-4	
$2^{-4}$	2.96722579697928E-5	3.3282
$2^{-5}$	2.05768964178787E-6	3.8500
$2^{-6}$	1.43249797801559E-7	3.8444

TABLE 4. The rate of convergence of first non-zero eigenvalue using the Clough-Tocher split and  $k = 2$ 

a measurement of the closest to singular vertex in the mesh, i.e.,  $\Theta_{\min}$  is small if there exists a vertex in  $\mathcal{T}_h$  that falls on two “almost” straight lines; see (3.20) and (3.19) for the precise definition.

In the first series of tests, we numerical study the effect of  $\Theta_{\min}$  in the finite element method (1.2). To this end, we first take  $\mathcal{T}_h$  to be the criss-cross mesh with  $h = 1/6$  (cf. Figure 5). This triangulation has 36 singular vertices, but  $\Theta_{\min}$  is well-behaved. Theorems 2.4 and 3.13 indicate that the finite element scheme (1.2) (with quartic Lagrange elements) leads to accurate approximations. Indeed, Table 5 lists the first ten computed non-zero eigenvalues, and it clearly shows accurate results.

Next, we perform the same tests but randomly perturb each singular vertex of the criss-cross mesh by a factor  $\alpha h$  for some  $\alpha \in (0, 1]$ . In particular, for each singular vertex  $z \in \mathcal{S}_h$  of the criss-cross triangulation  $\mathcal{T}_h$ , we make the perturbation  $z \rightarrow z + (\pm \alpha h, \pm \alpha h)$ . Figures 5(right), 4(left), and 4(right) show the resulting triangulations with  $\alpha = 0.01$ ,  $\alpha = 0.05$ , and  $\alpha = 0.1$ , respectively. We note that on

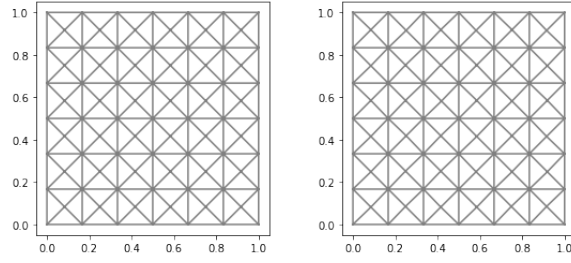


FIGURE 3. Left: Criss-cross mesh with  $h = 1/6$ . Right: The mesh obtained by randomly perturbing the singular vertices of the criss-cross mesh by  $0.01h$ .

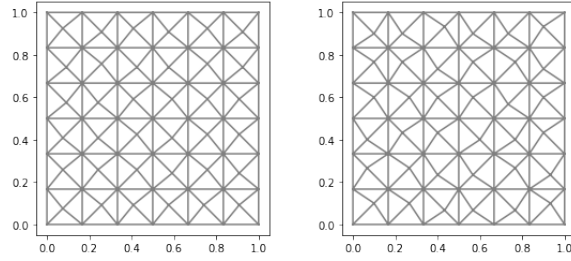


FIGURE 4. Criss-cross meshes with singular vertices randomly perturbed by  $0.05h$  (left) and  $0.1h$  (right).

the resulting perturbed mesh,  $\Theta_{\min} \approx \alpha$ , and therefore Theorem 3.13 suggests that the finite element approximation (1.2) may suffer for small  $\alpha$ -values.

The computed eigenvalues, with values  $\alpha = 0.01$ ,  $\alpha = 0.05$ , and  $\alpha = 0.1$ , are reported in Tables 6, 7, and 8, respectively. Table 8 shows that, for relatively large perturbations ( $\alpha = 0.1$ ), we compute relatively accurate eigenvalue approximations with similar convergence properties found on the criss-cross mesh (cf. Table 5). On the other hand, for smaller perturbations ( $\alpha = 0.05$  and  $\alpha = 0.01$ ), the results drastically differ. Table 6 clearly show extremely poor approximations for all eigenvalues, and Table 7 only computes the first few eigenvalues with reasonable accuracy before the results deteriorate. These numerical tests indicate the approximation properties of the computed eigenvalues are highly sensitive to the quantity  $\Theta_{\min}$ .

$i$	$\lambda_h^{(i)}$	$ \lambda^{(i)} - \lambda_h^{(i)} $
1	9.869604401309	2.199112003609E-10
2	9.869604401309	2.200408744102E-10
3	19.73920880459	2.414715538634E-09
4	39.47841782951	2.251546860066E-07
5	39.47841782951	2.251547499554E-07
6	49.34802238840	3.829525141441E-07
7	49.34802238840	3.829534165334E-07
8	78.95683762620	2.417486058448E-06
9	88.82645223886	1.262905662713E-05
10	88.82645223886	1.262905958299E-05

TABLE 5. Approximate eigenvalues using quartic Lagrange elements on a criss-cross mesh with  $h = 1/6$ .

$i$	$\lambda_h^{(i)}$	$ \lambda^{(i)} - \lambda_h^{(i)} $
1	1.424154538647	8.445449862442
2	1.471404605901	8.398199795188
3	1.477776343297	18.26143245888
4	1.502342236815	37.97607536754
5	1.526468793982	37.95194881038
6	1.540736126805	47.80728587864
7	1.552154885100	47.79586712035
8	1.556952619119	77.39988258960
9	1.566640464185	87.25979914562
10	1.580713040988	87.24572656882

TABLE 6. Approximate eigenvalues using quartic Lagrange elements on a  $0.01h$ -perturbed criss-cross mesh with  $h = 1/6$ .

$i$	$\lambda_h^{(i)}$	$ \lambda^{(i)} - \lambda_h^{(i)} $
1	9.869604401311	2.212932059820E-10
2	9.869604401311	2.215134742301E-10
3	19.73920880479	2.614239491550E-09
4	35.63498774612	3.843429858239
5	36.48359498561	2.994822618752
6	36.92351459416	12.42450741128
7	37.63299206644	11.71502993900
8	37.78514981304	41.17168539568
9	38.10084364520	50.72559596460
10	38.35191236801	50.47452724179

TABLE 7. Approximate eigenvalues using quartic Lagrange elements on a  $0.05h$ -perturbed criss-cross mesh with  $h = 1/6$ .

$i$	$\lambda_h^{(i)}$	$ \lambda^{(i)} - \lambda_h^{(i)} $
1	9.869604401320	2.310134306071E-10
2	9.869604401320	2.312834368468E-10
3	19.73920880546	3.285371974471E-09
4	39.47841784038	2.360199999885E-07
5	39.47841784071	2.363495781310E-07
6	49.34802242662	4.211773898533E-07
7	49.34802246288	4.574410894520E-07
8	78.95683842488	3.216167357323E-06
9	88.82645270371	1.309390694360E-05
10	88.82645276747	1.315766178323E-05

TABLE 8. Approximate eigenvalues using quartic Lagrange elements on a  $0.1h$ -perturbed criss-cross mesh with  $h = 1/6$ .

**4.4. Quartic Lagrange elements on generic triangulations.** Our next series of tests compute the finite element method (1.2) using quartic Lagrange elements on generic Delaunay triangulations. Again, Theorem 3.13 and the previous set of tests indicate the approximation properties of the computed eigenvalues are highly sensitive to the quantity  $\Theta_{\min}$ . In light of this, for a given (generic)



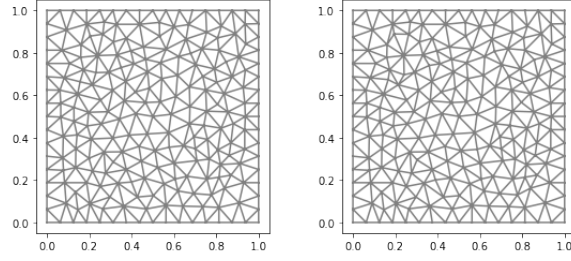


FIGURE 5. (left) Unstructured mesh with  $h \approx 1/10$ , (right) randomly perturbing interior vertices who have four triangles by at most  $.1h$

triangulation  $\mathcal{T}_h$  we randomly move each interior vertex with four neighboring triangles by a  $0.1h$ -perturbation; see Figure 5.

Table 10 shows the maximum errors of the first 20 computed eigenvalues on these perturbed mesh for  $h = 2^{-j}$  ( $j = 2, 3, 4, 5$ ). The table clearly shows convergence with rate  $\mathcal{O}(h^8)$ . On the other hand, the errors of the computed eigenvalues on ‘non-perturbed’ meshes do not converge as shown in Table 9.

$h$	$\max_{1 \leq i \leq 20}  \lambda^{(i)} - \lambda_h^{(i)} $	rate
$2^{-2}$	8.38611345105E-03	
$2^{-3}$	5.61831120933E-05	7.2217
$2^{-4}$	59.2176263988	-20.008
$2^{-5}$	59.2176264065	0.000

TABLE 9. Maximum error of the first 20 eigenvalues on (non-perturbed) Delaunay triangulations using quartic Lagrange elements. Note that for  $h = 2^{-2}$  and  $h = 2^{-3}$ , the mesh  $\mathcal{T}_h$  does not have any vertices with four neighboring triangles.

$h$	$\max_{1 \leq i \leq 20}  \lambda^{(i)} - \lambda_h^{(i)} $	rate
$2^{-2}$	8.3861134511E-03	
$2^{-3}$	5.6183112093E-05	7.2217
$2^{-4}$	2.2360291041E-07	7.9731
$2^{-5}$	8.9832496997E-10	7.9595

TABLE 10. Maximum error of the first 20 eigenvalues on perturbed Delaunay triangulations using quartic Lagrange elements.

#### APPENDIX A. PROOF OF LEMMA 3.1

The construction of an interpolant  $\mathbf{I}_h : \mathring{\mathbf{V}} \rightarrow \mathcal{P}_1^c(\mathcal{T}_h) \cap \mathbf{H}_0(\text{rot}, \Omega)$  satisfying (3.1) is similar to the original Scott–Zhang interpolant in [23] (also see [9]), but slightly modified at the corners of the domain  $\Omega$ .

For each vertex  $z \in \mathcal{V}_h$ , let  $e_z \in \mathcal{E}_h$  be an arbitrary edge such that  $z \in \bar{e}_z$ . If  $z$  is a boundary vertex, then we require that  $e_z \in \mathcal{E}_h^B$ . Let  $\{a_z^{(1)}, a_z^{(2)}\}$  be the end points of  $e_z$  with  $z = a_z^{(1)}$ . Let  $\{\phi_z^{(1)}, \phi_z^{(2)}\}$  be the (scalar) piecewise linear function satisfying  $\phi_z^{(i)}(a_z^{(j)}) = \delta_{i,j}$ , set  $\phi_z := \phi_z^{(1)}$ , and let  $\{\psi_z^{(1)}, \psi_z^{(2)}\}$  be a dual basis satisfying

$$\int_{e_z} \psi_z^{(i)} \phi_z^{(j)} = \delta_{i,j}, \quad \text{and} \quad \psi_z := \psi_z^{(1)}.$$

For  $\delta > 0$ , the modified Scott–Zhang interpolant is then defined as the operator  $\mathbf{I}_h : \mathring{\mathbf{V}} \rightarrow \mathcal{P}_1^c(\mathcal{T}_h) \cap \mathbf{H}_0(\text{rot}, \Omega)$  given by

$$\mathbf{I}_h \boldsymbol{\tau}(x) = \sum_{z \in \mathcal{V}_h \setminus \mathcal{V}_h^C} \phi_z(x) \int_{e_z} \psi_z \boldsymbol{\tau},$$

where multiplication and integration is performed component-wise. Recall that if  $z \in \mathcal{V}_h^B$ , then  $e_z \in \mathcal{E}_h^B$ , and therefore  $(\mathbf{I}_h \boldsymbol{\tau}(z)) \cdot \mathbf{t}_{e_z} = 0$  for all  $z \in \mathcal{V}_h^B$ . Here,  $\mathbf{t}_{e_z}$  is a (constant) unit tangent vector of the edge  $e_z$ . We then conclude that  $\mathbf{I}_h \boldsymbol{\tau} \cdot \mathbf{t}|_{\partial\Omega} = 0$ . We further note that  $(\mathbf{I}_h \boldsymbol{\tau})(z) = 0$  for all  $z \in \mathcal{V}_h^C$ .

The canonical Scott–Zhang interpolant is [23]

$$\tilde{\mathbf{I}}_h \boldsymbol{\tau}(x) := \sum_{z \in \mathcal{V}_h} \phi_z(x) \int_{e_z} \psi_z \boldsymbol{\tau},$$

and so

$$\tilde{\mathbf{I}}_h \boldsymbol{\tau}(x) - \mathbf{I}_h \boldsymbol{\tau}(x) = \sum_{z \in \mathcal{V}_h^C} \phi_z(x) \int_{e_z} \psi_z \boldsymbol{\tau}.$$

We then conclude that  $\tilde{\mathbf{I}}_h \boldsymbol{\tau} = \mathbf{I}_h \boldsymbol{\tau}$  on all  $T \in \mathcal{T}_h$  such that  $T \not\in \mathcal{T}_h(z)$  for all  $z \in \mathcal{V}_h^C$ . Therefore (3.1) is satisfied by properties of the canonical Scott–Zhang interpolant. Thus, it suffices to prove (3.2).

Let  $T \in \mathcal{T}_h(z)$  for some  $z \in \mathcal{V}_h^C$ . A standard scaling argument shows

$$\|\tilde{\mathbf{I}}_h \boldsymbol{\tau} - \mathbf{I}_h \boldsymbol{\tau}\|_{L^2(T)} \leq Ch_T^2 \left| \int_{e_z} \psi_z \boldsymbol{\tau} \right|^2,$$

and  $\|\psi_z\|_{L^\infty(e_z)} \leq Ch_T^{-1}$ . Hence, there holds

$$\|\tilde{\mathbf{I}}_h \boldsymbol{\tau} - \mathbf{I}_h \boldsymbol{\tau}\|_{L^2(T)}^2 \leq C \|\boldsymbol{\tau}\|_{L^1(e_z)}^2 \leq Ch_T \|\boldsymbol{\tau}\|_{L^2(e_z)}^2.$$

Now suppose that  $\boldsymbol{\tau}$  is smooth. Then, since  $\boldsymbol{\tau} \cdot \mathbf{t}|_{\partial\Omega} = 0$ , there holds  $\boldsymbol{\tau}(z) = 0$  on  $z \in \mathcal{V}_h^C$ . Therefore  $\|\boldsymbol{\tau}\|_{L^2(e_z)} \leq Ch_T^\delta \|\boldsymbol{\tau}\|_{H^\delta(e_z)} \leq Ch_T^\delta \|\boldsymbol{\tau}\|_{H^{1/2+\delta}(\Omega)}$  by a Poincaré inequality and a trace inequality [13].

For a general  $\boldsymbol{\tau} \in \mathring{\mathbf{V}}$ , let  $\{\boldsymbol{\tau}_n\}_{n=1}^\infty \subset \mathbf{C}^\infty(\Omega) \cap \mathbf{H}_0(\text{rot}, \Omega)$  satisfy  $\lim_{n \rightarrow \infty} (\|\boldsymbol{\tau} - \boldsymbol{\tau}_n\|_{H(\text{rot}, \Omega)} + \|\boldsymbol{\tau} - \boldsymbol{\tau}_n\|_{H(\text{div}, \Omega)}) = 0$ . This is possible since the space  $\mathbf{C}^\infty(\Omega) \cap \mathbf{H}_0(\text{rot}, \Omega)$  is dense in  $\mathring{\mathbf{V}}$ ; the density result was proved in [11] (see also the beginning of the proof of Theorem 2.3 in [10]). Further note that  $\lim_{n \rightarrow \infty} \|\boldsymbol{\tau} - \boldsymbol{\tau}_n\|_{H^{1/2+\delta}(\Omega)} = 0$ . We then have

$$\begin{aligned} \|\boldsymbol{\tau}\|_{L^2(e_z)} &\leq \|\boldsymbol{\tau} - \boldsymbol{\tau}_n\|_{L^2(e_z)} + \|\boldsymbol{\tau}_n\|_{L^2(e_z)} \\ &\leq C(\|\boldsymbol{\tau} - \boldsymbol{\tau}_n\|_{H^{1/2+\delta}(\Omega)} + h_T^\delta \|\boldsymbol{\tau}_n\|_{H^{1/2+\delta}(\Omega)}) \\ &\leq C(h_T^\delta \|\boldsymbol{\tau}\|_{H^{1/2+\delta}(\Omega)} + \|\boldsymbol{\tau} - \boldsymbol{\tau}_n\|_{H^{1/2+\delta}(\Omega)}) \\ &\rightarrow Ch_T^\delta \|\boldsymbol{\tau}\|_{H^{1/2+\delta}(\Omega)} \quad \text{as } n \rightarrow \infty. \end{aligned}$$

Therefore

$$\|\tilde{\mathbf{I}}_h \boldsymbol{\tau} - \mathbf{I}_h \boldsymbol{\tau}\|_{L^2(T)}^2 \leq Ch_T^{1+2\delta} \|\boldsymbol{\tau}\|_{H^{1/2+\delta}(\Omega)}^2.$$

Finally, we use the triangle and inverse inequalities and standard properties of the Scott–Zhang interpolant:

$$\begin{aligned} \|\boldsymbol{\tau} - \mathbf{I}_h \boldsymbol{\tau}\|_{L^2(T)} &\leq \|\boldsymbol{\tau} - \tilde{\mathbf{I}}_h \boldsymbol{\tau}\|_{L^2(T)} + \|\mathbf{I}_h \boldsymbol{\tau} - \tilde{\mathbf{I}}_h \boldsymbol{\tau}\|_{L^2(T)} \leq Ch^{1/2+\delta} \|\boldsymbol{\tau}\|_{H^{1/2+\delta}(\Omega)}, \\ \|\mathbf{I}_h \boldsymbol{\tau}\|_{H^{1/2+\delta}(T)} &\leq h_T^{-1/2-\delta} \|\mathbf{I}_h \boldsymbol{\tau} - \tilde{\mathbf{I}}_h \boldsymbol{\tau}\|_{L^2(T)} + \|\tilde{\mathbf{I}}_h \boldsymbol{\tau}\|_{H^{1/2+\delta}(T)} \leq C \|\boldsymbol{\tau}\|_{H^{1/2+\delta}(\Omega)}. \end{aligned}$$

## REFERENCES

- [1] M. S. Alnaes, J. Blechta, J. Hake, A. Johansson, B. Kehlet, A. Logg, C. Richardson, J. Ring, M. E. Rognes and G. N. Wells, *The FEniCS Project Version 1.5*, Archive of Numerical Software, vol. 3, 2015.
- [2] C. Amrouche, C. Bernardi, M. Dauge, and V. Girault, *Vector potential in three dimensional nonsmooth domains*, Math. Methods Appl. Sci., 21:823–864, 1998.
- [3] D.N. Arnold, R.S. Falk, and R. Winther, *Finite element exterior calculus: from Hodge theory to numerical stability*, Bull. Amer. Math. Soc. (N.S.), 47(2):281–354, 2010.
- [4] I. Babuška and J. Osborn, *Eigenvalue Problems*, in Handbook of Numerical Analysis, II:641–787, North-Holland, Amsterdam, 1991.
- [5] D. Boffi, *Finite element approximation of eigenvalue problems*, Acta Numer., 1–120, 2010.
- [6] D. Boffi, F. Brezzi, and L. Gastaldi, *On the problem of spurious eigenvalues in the approximation of linear elliptic problems in mixed form*, Math. Comp., 69(229):121–140, 2000.
- [7] D. Boffi, F. Brezzi, L. Demkowicz, R.G. Durán, R.S. Falk, and M. Fortin, *Mixed finite elements, compatibility conditions, and applications*, Lectures given at the C.I.M.E. Summer School held in Cetraro, June 26?July 1, 2006. Edited by Boffi and Lucia Gastaldi. Lecture Notes in Mathematics, 1939. Springer-Verlag, Berlin; Fondazione C.I.M.E., Florence, 2008.
- [8] D. Boffi, P. Fernandes, L. Gastaldi, and I. Perugia, *Computational models of electromagnetic resonators: analysis of edge element approximation*, SIAM J. Numer. Anal., 36(4):1264–1290, 1999.
- [9] P. Ciarlet, *Analysis of the Scott–Zhang interpolation in the fractional order Sobolev spaces*, J. Num. Math., 21(3):173–180, 2013.
- [10] M. Costabel and M. Dauge, *Maxwell and Lamé eigenvalues on polyhedra*, Math. Meth. Appl. Sci., 22:243–258, 1999.
- [11] M. Costabel, M. Dauge, and S. Nicaise, *Singularities of Maxwell interface problems*, Math. Modell. Numer. Anal., 33:627–649, 1999.
- [12] H. Duan, Z. Du, W. Liu and S. Zhang, *New Mixed Elements for Maxwell Equations*, SIAM J. Numer. Anal., 57(1):320–54, 2019.
- [13] T. Dupont and R. Scott, *Polynomial approximation of functions in Sobolev spaces*, Math. Comp. 34:441–463, 1980.
- [14] R. Falk and M. Neilan, *Stokes complexes and the construction of stable finite element methods with pointwise mass conservation*, SIAM J. Numer. Anal., 51(2):1308–1326, 2013.
- [15] G. Fu, J. Guzman, and M. Neilan, *Exact smooth piecewise polynomial sequences on Alfled splits*, Math. Comp., 89(323):1059–1091, 2020.
- [16] J. Guzman, A. Lischke, and M. Neilan, *Exact sequences on Powell–Sabin splits*, submitted.
- [17] J. Guzman and R. Scott, *The Scott–Vogelius finite elements revisited*, Math. Comp., 88(316):515–529, 2019.
- [18] T. Kato, *Perturbation theory for linear operators*, Reprint of the 1980 edition. Classics in Mathematics. Springer-Verlag, Berlin, 1995.
- [19] M.-J. Lai and L. L. Schumaker, *Spline functions on triangulations*, Encyclopedia of Mathematics and its Applications, 110., Cambridge University Press, Cambridge, 2007
- [20] M. J. D. Powell and M. A. Sabin, *Piecewise quadratic approximations on triangles*, ACM Trans. Math. Software 3(4):316–325, 1977.
- [21] J. Qin, *On the convergence of some low order mixed finite elements for incompressible fluids*, Ph.D. Thesis, The Pennsylvania State University, 1994.
- [22] L. R. Scott and M. Vogelius, *Norm estimates for a maximal right inverse of the divergence operator in spaces of piecewise polynomials*, RAIRO Model. Math. Anal. Numer. 19(1):111–143, 1985.
- [23] L. R. Scott and S. Zhang, *Finite element interpolation of non smooth functions satisfying boundary conditions*, Math. Comp., 54(190):483–493, 1990.
- [24] S. H. Wong and Z. J. Cendes, *Combined finite element-modal solution of three-dimensional eddy current problems*, IEEE Transactions on Magnetism, 24(6):2685–2687, 1988.

KING ABDULLAH UNIVERSITY OF SCIENCE AND TECHNOLOGY, SAUDI ARABIA AND UNIVERSITY OF PAVIA, ITALY  
*E-mail address:* `daniele.boffi@kaust.edu.sa`

DIVISION OF APPLIED MATHEMATICS, BROWN UNIVERSITY  
*E-mail address:* `johnny.guzman@brown.edu`

DEPARTMENT OF MATHEMATICS, UNIVERSITY OF PITTSBURGH  
*E-mail address:* `neilan@pitt.edu`